Comparison of 3 self-starting step-up DC:DC converter topologies for harvesting energy from low-voltage and low-power microbial fuel cells

Nicolas Degrenne, Bruno Allard, François Buret, Florent Morel, Salah-Eddine Adami, Denis Labrousse

Comparison of 3 Self-Starting Step-Up DC:DC Converter Topologies for Harvesting Energy from Low-Voltage and Low-Power Microbial Fuel Cells

Nicolas Degrenne[1], Bruno Allard[2], François Buret[1], Florent Morel[1],
Salah-Eddine Adami[1], Denis Labrousse[1]
Université de Lyon, Ecole Centrale de Lyon, INSA Lyon, Laboratoire Ampère, UMR 5005
36 avenue Guy de Collongue, 69130 Ecully, France
E-Mail: [1]firstname.surname@ec-lyon.fr, [2]firstname.surname@insa-lyon.fr

Keywords

«Fuel cell system», , «switched-mode power supply», «alternative energy», «resonant converter».

Abstract

This paper describes and evaluates 3 original step-up converter architectures able to harvest energy from low-voltage and low-power generators. Design and sizing are made according to specifications issued from the stringent characteristics of microbial fuel cells. The maximum harvested power is 10mW under input voltage Vin=0.3V (33mA input current). The considered converters include self-oscillating circuits for autonomous operation. The 2 first topologies are respectively adapted from boost and flyback topologies. The 3rd topology uses a Greinacher voltage-lift circuit. Energy is transferred to the load both directly (forward transfer) and indirectly (flyback transfer). PSPICE simulations enable evaluation and comparison of the 3 topologies in term of efficiency, robustness, step-up ratio, control and cost. Best efficiency of 80.6% is achieved by the boost-derived circuit which also enables a feedback action to harvest energy at maximum power point.

Introduction

Energy harvesting is the process by which energy is captured from environment and stored or used to feed low-power circuits (e.g. network of wireless autonomous sensors). It is an alternative to environmentally harmful and life-limited batteries in embedded systems. Kinetic, thermal, solar, and electromagnetic energy can be transformed into electricity using appropriate harvesting transducers (respectively piezoelectric, thermoelectric, photovoltaic and special antennas) [1]. As shown in table I, most harvesting devices produce low power under low maximum power point (MPP) voltages.

Table I: Harvesting devices comparison (estimations based on various papers including [2])

Harvester	Condition	Power density	Power cost	MPP Voltage
Photovoltaic	indoor	10 µW/cm^2	1 €/mW	0.5V
	outdoor	10 mW/cm^2	0.001 €/mW	0.5V
Mechanical	piezoelectric	300 µW/cm^3	50 €/mW	> 5V
	electrostatic	10 µW/cm^3	>100 €/mW	> 5V
	electromagnetic	100 µW/cm^3	50 €/mW	< 0.5V
Thermal	body (5 °C)	50 µW/cm^2	100 €/mW	0.5V
	industry	1-10 mW/cm^2	2 €/mW	> 1V
Microwave	ambient (WiFi)	1 µW/cm^2	1000 €/mW	0.1V
Organic	microbial fuel cell	1 µW/cm^3	50 €/mW	0.3V

Microbial Fuel Cells (MFCs) produce electrical energy from organic matter via bacterial metabolisms [3]. These devices are basically composed of an anode and a cathode immersed in an electrolyte containing the fuel (Fig. 1). Domestic waste water can be used to feed microbial fuel cells, leading to its decontamination. Like most energy harvesters, they provide very small amount of power (presently about 1mW for a 1-liter single-chamber fuel cell) under low-voltage (0.3V). Internal presence and nature of substrate and bacteria is inconstant and uncontrollable but has a strong influence on cells equivalent internal serial resistance. These inevitable dispersions (maximum power is obtained at different currents for each cell) make it inefficient to associate cells in series [4] so we must rely on individual power conversion (namely step-up converters).

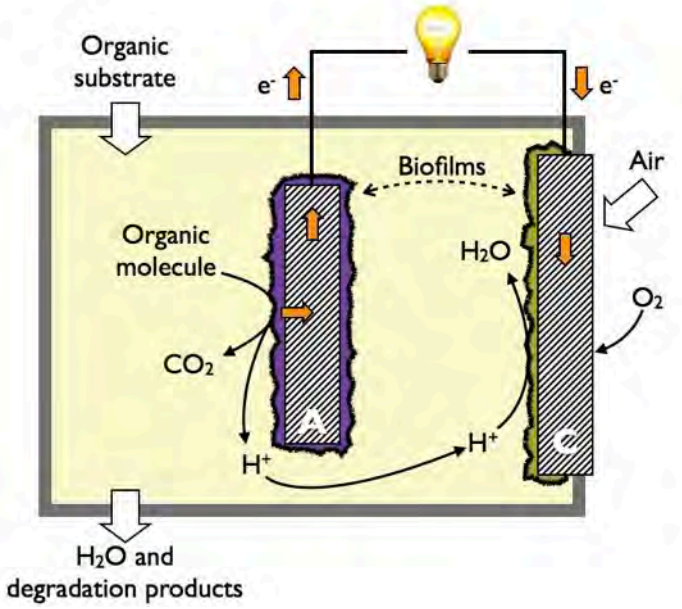

Fig. 1: Schematic diagram of a single chamber MFC

Low-voltage and low-power converters require specific design attention. Kimball, in [5], emphasizes start-up and efficiency issues. Most silicon components do not switch at gate voltages below 0.5V. Once in operation, the output voltage of the step-up converter can be sufficiently high to power the control circuit. If the output voltage is initially low, specific start-up topologies need to be implemented like in DC:DC converters compared Table II.

A first option is to realize the start-up circuit independently from the main DC:DC converter. The advantage is to permit the use of a classical high-efficiency main DC:DC converter. In [6], [7] and [8], the boost topology was respectively implemented with a charge-pump, mechanical, and transformer-based start-up.

A second option is to merge the start-up and the main circuit in order to decrease the number of components and the cost. Respectively boost and flyback architectures were presented in [9] and [10]. These two structures are respectively close to top1 and top2 studied in this paper.

A third option is to design new architectures especially built for low-voltage and low-power. The architecture presented in [11] is a transformer-based oscillating structure connected with a voltage doubler circuit. It transfers energy both directly and indirectly. This topology has gain interest recently in energy harvesting applications [12-13]. It is very similar to top3 studied in the present paper.
The present paper analyzes 3 step-up converter topologies customized for autonomous operation and sized for harvesting energy from MFCs. They include a circuit based on the association of a transformer which secondary winding controls a switch that is serially connected to the primary winding. This association ensures a positive feedback and sustained oscillations. In order to initiate operation, a normally-ON JFET is used as a switch.

Top1 and top2 are respectively modified boost and flyback converters. A self-starting and self-oscillating command was added through the use of an additional winding. In this paper, top3 is

referred to as «oscillator voltage-lifted topology». The input DC voltage is switched to an AC voltage at the secondary winding of the transformer. A high turn-ratio contributes to high amplitude of the AC voltage which is then rectified using an output Greinacher voltage lift. The present paper intends to unveil these 3 original harvesting converters. First, a description of microbial fuel cells is given. Specifications for the converters are deduced. Then, the 3 circuits are extensively described and operations principles are detailed. Circuits pros and cons are discussed and compared in term of efficiency, step-up ratio, circuit complexity, robustness and control ease.

Table II: Harvesting DC:DC converters comparison

Circuit	Start-up Voltage	Power range	Vout	MPPT	Output regulation	Peak efficiency
Linear technologies LTC310 (1:20) [12]	100mV	100µW to 100mW	2.35V to 5V	no	yes	0.6
Enocean ECT310 [14]	20mV	100µW to 100mW	3V to 5V	no	no	0.3
Seiko S-882Z [15]	300mV	? to 150µW	1.8V to 2.4V	no	yes	0.2
Markus [10]	70mV	200µ to 16mW	2V to 5V	no	yes	0.7
Qiu [16]	500mV	5µW to 10mW	0V to 5V	yes	yes	0.7
Ramadass [7]	35mV	10µW to ?	1.8V	yes	yes	0.58

Specifications

Microbial fuel cells's electrical characteristics can be assessed by different means including polarization curves, impedance spectroscopy, and tests under automatically controlled load [17-18]. These measurements offer precious information in order to design the harvesting power electronic module. For instance, for a 1-liter MFC (fig. 2) open circuit voltage is ≈0.6V, short-circuit current ≈6.6mA, internal serial resistance ≈90Ω and maximum power ≈1mW obtained for a MPP voltage ≈0.3V. Tests show that MFCs have a complex capacitive behavior. Recent works on multi-physical models [19] aim to link the electrical behavior to internal biological, physical, and electrochemical phenomena in order to achieve a global and multi-disciplinary understanding of MFCs. Other works [20] aim to describe the electrical behavior alone.

Fig. 2: Picture of 1-liter laboratory MFC

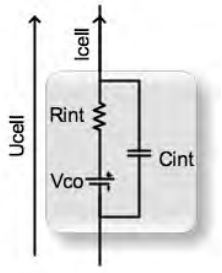

Fig. 3: Basic MFC electrical model

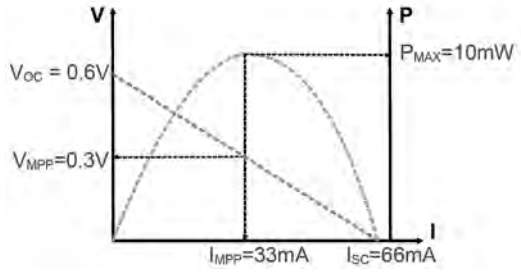

Fig. 4: Voltage and power curves for 10 1-liter MFCs connected in parallel

Converters presented in this paper are sized to harvest energy from 10 1-liter MFCs connected in parallel. MFCs are assumed to all correspond to the electrical model figure 4, leading to an equivalent circuit which open circuit voltage is ≈0.6V and internal serial resistance ≈90Ω (figure 4).

MFCs were tested under different fuel conditions, and it was found that open-circuit voltage is almost constant while the internal resistance Rint increases when fuel concentration decreases. For this reasons, we will test the converters with changing Rint conditions. The converter ideally includes maximum power point tracking (MPPT) function to harvest the maximum available power from the source regardless of its internal resistance. The output voltage is not to be regulated precisely, but must be above 1V in order to enable a second step-up stage to be realized in conventional CMOS technology.

Table III: Harvesting DC:DC converter specifications for MFCs

Description	Name	Unit	Min	Typical	Max
Input open-circuit voltage	Vin0	V	0.5	0.6	0.7
Input source serial resistance	Rint	Ω	3	9	45
Input regulated voltage	Vin	V	0.2	0.3	0.5
Efficiency	η		70 %		
Output voltage	Vout	V	1V		

Boost topology (top1)

Circuit architecture

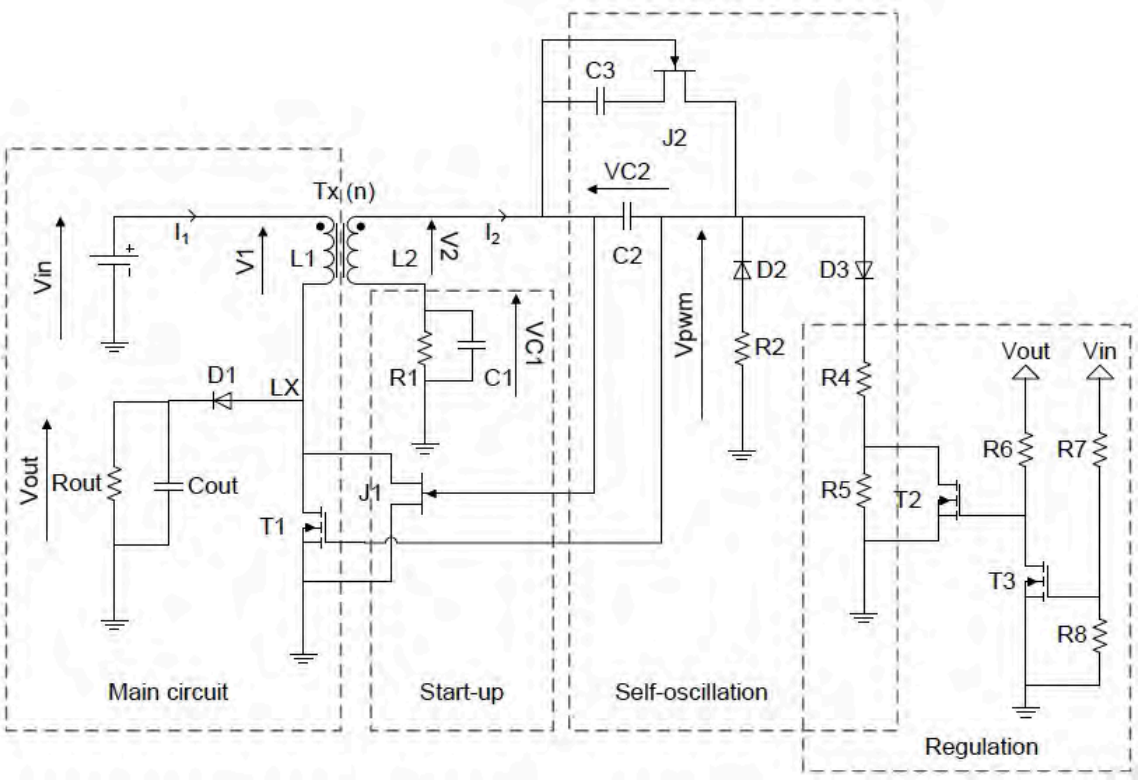

Fig. 5: schematic of top1 powered by ideal voltage source and loaded by a resistor

The converter presented Fig. 5 is based on a conventional boost converter like proposed in [10]. The main circuit inductor L_1 is coupled to L2 to feed start-up, self oscillating, and regulation circuits.

Table IV: Component values for top1

Part	Value	Part	Value	Part	Value	Part	Value
Vin	0.3V	R1	1 kΩ	C2	300 pF	R7	100 kΩ
Tx	WE749197301 (1:5)	C1	8 µF	C3	3 nF	R8	200 kΩ
D1	BAT54	J1	JBF862	J2	JBF862	T3	ALD110802
T1	DMG6968			R2	50 kΩ	R6	2 MΩ
Cout	8 µF			D2	HSMS285x	T2	ALD110802
Rout	1 kΩ			D3	HSMS285x	R5	500 kΩ
						R4	20 kΩ

The transformer SPICE model being unavailable, it was replaced by a linear transformer (L1=326.7µH, L2=8167µH, coupling K=0.999) with serial resistances R_{L1}=34 mΩ and R_{L2}=170 mΩ.

Circuit operation

Main boost circuit

The main circuit is an asynchronous boost converter operating at the boundary of the continuous and discontinuous mode (critical conduction mode). Ideal step-up ratio is given by equation (1), D being the duty cycle.

$$\frac{V_{OUT}}{V_{IN}} = \frac{1}{1-D} \tag{1}$$

Self-oscillation

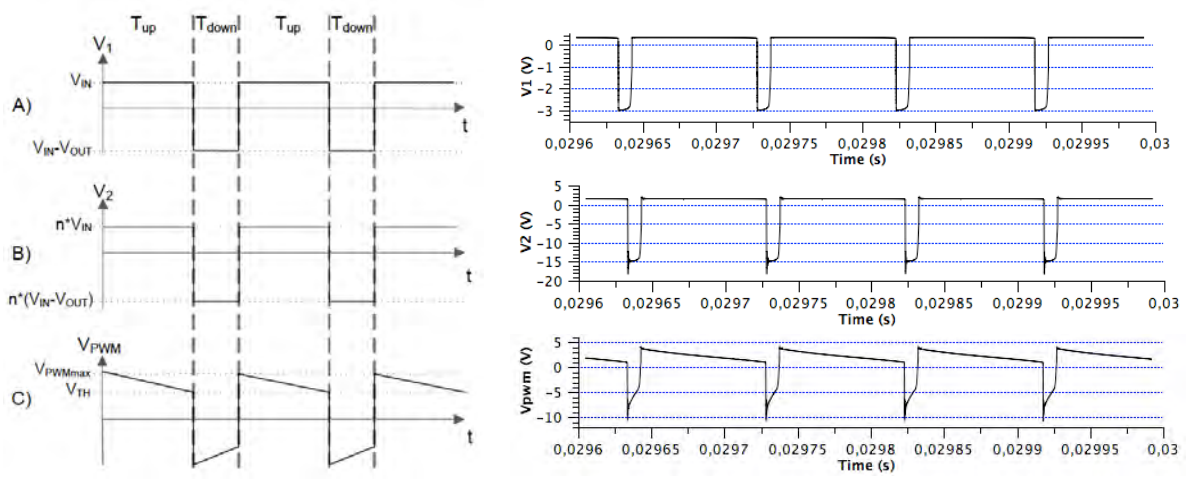

Fig. 6: Ideal and simulated signals for top1

The boost main switch T_1 is controlled by a pulse-width modulated signal V_{PWM}. During steady-state, the primary winding of the transformer is either subject to voltage $V_1=V_{IN}$ during T_1 ON-state (Tup), either to $V_1=V_{IN}-V_{OUT}$ during T_1 OFF-state (Tdown). If we consider L_1 and L_2 to be ideally coupled, $V_2=n*V_1$.

During Tup, $V_2=n*V_{IN}$ and V_{PWM} is positive (we assume $V_{C2}=0$). Diode D_3 is ON and the capacitor C_2 charges (V_{C2} increases) in the equivalent serial resistance (to D_3) with defined time constant. When the voltage V_{PWM} reaches the threshold voltage V_{TH} of T_1, it turns OFF.

During Tdown, diode D_2 is ON. The capacitor C2 discharges (V_{C2} decreases) through R_2. Tdown lasts until the current through the diode D_1 decreases to zero and cancels. I1 gets negative (through the body-diode of T_1), lowers the LX node voltage and inverts voltage V_1 at the primary winding of the transformer.

When D_3 is ON again (Tup), the initial PWM voltage (V_{PWMMAX}) will be higher than V_{TH} because V_{C2} decreased during Tdown.

Regulation

The regulation loop controls the input voltage V_{IN}. It modifies the equivalent resistance (serially connected to D_3) that sets Tup and the switching frequency (f ≈ 10kHz for Rint = 9Ω). Transistor T_3 is a specific ultra-low voltage NMOS transistor. T_3 drives transistor T_2 through a logic-inverter structure (R_6 and T_3) which is powered from the output voltage of the converter. Resistors R_4 and R_5 are necessary to adapt minimum and maximum values of the equivalent serial resistance.

Start-up

JFET J_1 is connected in parallel with NMOS T_1 and enables autonomous start-up. When a positive voltage V_{IN} is applied at the input, the current I_1 through the primary winding and through the normally-ON JFET T_1 increases. The voltage V_2=n*V_1 (n=n_2/n_1=5 turn-ratio) at the secondary winding is positive. Since the gate of T_1 is biased positively (initially V_{C1}=0), the internal diode of T_1 conducts and the V_{C1} gets negative. When the current I_1 is high enough, V_1 decreases (RL time constant), and V_2 decreases. The gate voltage of J_1 therefore decreases, and its ON-resistance increases. J_1 is driven slightly towards the off-state.

When J_1 is OFF, the current I_1 decreases through D_1. V_1 and V_2 get negative. When I_1 gets negative, voltage V_1 increases, V_2 increases and T_1 switches ON again. Oscillations amplify and the output capacitor C_3 is charged, amplifying the current slopes. At a certain point, the amplitude of oscillations is high enough and T_1 switches ON and OFF synchronously with J_1. When the voltage across C_1 is negative enough, J_1 stops switching.

Flyback topology (top2)

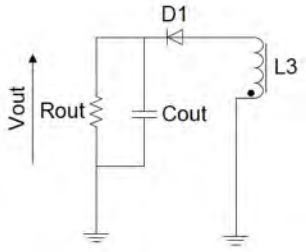

Fig. 7: Output winding schematic of flyback converter (top2).

Converter in Fig. 7 is a modified flyback converter. The schematic is identical to the boost schematic except that D_1's anode is not connected to the LX node but to a 3rd coupled winding presented figure 6 (n_2/n_1=4, n_3/n_1=1). Its operation is very similar to operation of top1.

Flyback step-up ratio (2) potentially enables high step-up if a large turn-ratio n_3/n_1 is used. This structure also potentially permit the output to be isolated (different output ground), which is advantageous in order to connect the outputs of several similar converters in series. In the presented converter however, the 2nd winding is both connected to V_{IN} and V_{OUT} to enable proper regulation, and insulation is therefore not permitted. Flyback topology requires a complex transformer structure with 3 windings, each ideally with different turn-ratios. In flyback operation, the current in the transformer is subject to discontinuities which impose the need of a very high coupling coefficient between windings 1 and 3.

$$\frac{V_{OUT}}{V_{IN}} = \frac{n_3}{n_1} * \frac{D}{1-D} \quad (2)$$

Oscillator voltage-lifted topology (top3)

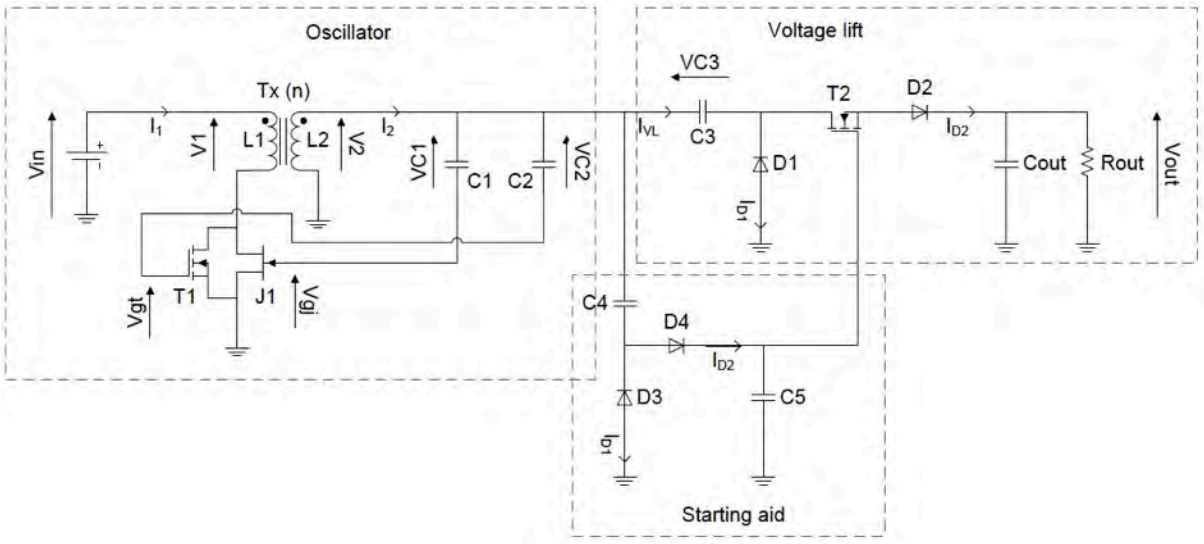

Fig. 8: Schematic of top3 powered by ideal voltage source and loaded by a resistor

The converter presented figure 8 is not derived from a classical power electronics structure. It is composed of a transformer based high step-up oscillator, a Greinacher voltage-lift circuit, and a starting aid circuit.

Table V: Component values for top3

Parts	Value	Parts	Value	Parts	Value
Vin	0.3 V	C4	300 pF	C3	8 nF
Tx	WE749196510 (1:5)	D3	BAT54	D1	BAT54
T1	DMG6968	D4	BAT54	T2	DMG6968
J1	JBF862	C5	100 nF	D2	BAT54
C1	100 pF			Cout	500 nF
C2	1 nF			Rout	1 kΩ

The transformer SPICE model being unavailable, it was replaced by a linear transformer (L1=9.9µH, L2=247.5µH, coupling=0.982) with serial resistances R_{L1}=30 mΩ and R_{L2}=150 mΩ.

Circuit operation

Oscillator

The start-up mechanism is similar to the one of top1 and top2. J_1 initiates the oscillation and T_1 enable high-efficiency operation during steady-state. During Tup, T_1 is ON. Primary voltage V_1 is imposed. The current in the magnetizing inductor increases. V_1 decreases with a RL time constant (T_{RL}). When the gate voltage of T_1 reaches threshold voltage, it turns OFF. The ON-time duration is close to T_{RL}. During Tdown, the circuit exhibits a RLC behavior. The inductance is L_2 and the equivalent capacitance is mainly function of C_1, C_2, C_3, C_4, and gates capacitances of T_1 and J_1 (C_3 dominates). This circuit oscillates. Initial energy is mainly delivered by the current stored in the magnetizing inductance during the ON state. Voltages V_1 and V_2 get very negative and positive again, causing J_1 to turn ON again. The OFF time duration is half the RLC time constant (T_{RLC}). Observed frequency is about 100kHz.

This favorable circuit behavior is true only if $\alpha*T_{RL}>T_{RLC}$ (α constant). Otherwise, $T_{up}=T_{down}=T_{RLC}/2$. In this case, there is very little energy stored in the magnetizing inductance, and there is a much lower negative voltage amplitude during Tdown.

Greinacher voltage lift

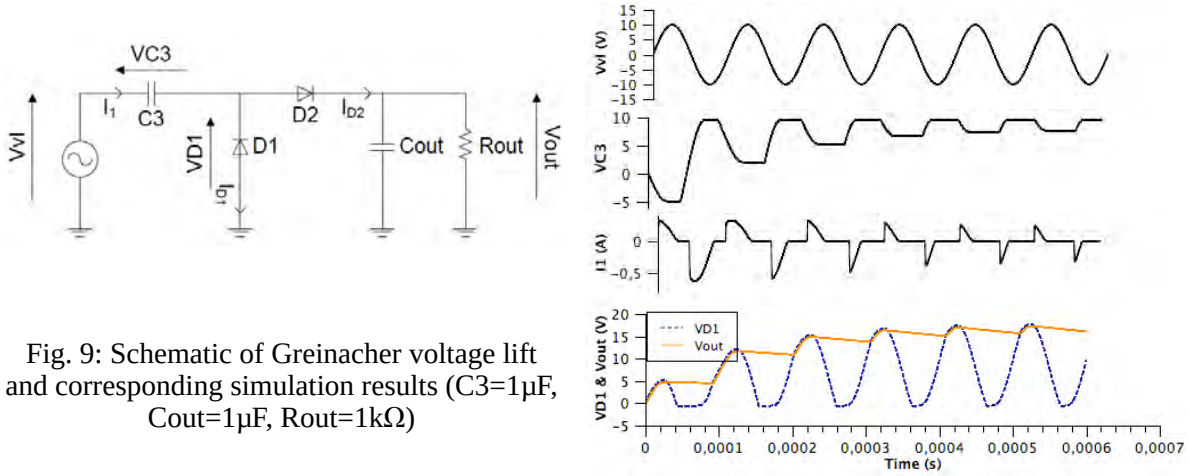

Fig. 9: Schematic of Greinacher voltage lift and corresponding simulation results (C3=1µF, Cout=1µF, Rout=1kΩ)

During the first negative half period of V_{VL}, a negative current I_1 (D_1 is ON) charges C_3 to a voltage $V_{C3}=V_{IN}$. When the voltage V_{IN} increases above $V_{OUT}-V_{C3}$, C_3 partly discharge through D_2 (positive current I_1). During the next negative half period, a negative I_{D1} current partly charges C3 again. C3 is a pump capacitor. Output voltage is almost equal to V_{VL} peak to peak amplitude voltage.

Starting aid

The starting aid circuit disconnects the load from the oscillator during start-up in order to temporarily decrease the apparent secondary equivalent capacitance and ensure $T_{RL}>T_{RLC}$ even during start-up when only J_1 switches.

Performance evaluation

Simulation methodology

All these 3 topologies are simulated (SPICE) using circuit-level discrete models together with MFC basic electrical equivalent model. Circuits are tested under different MFC internal resistance (Rint). Top2 results are very close to top1 results and are not shown.

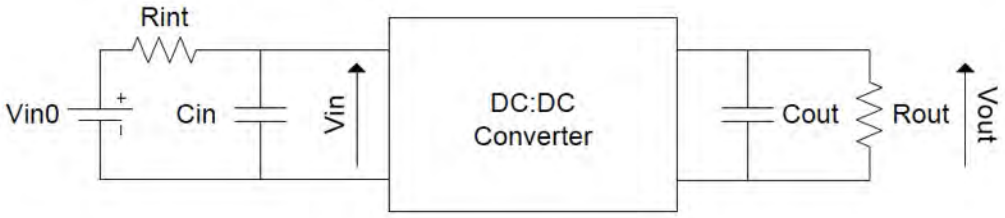

Fig. 10: Test of harvesting converters with MFCs basic electrical model

Discussion

In this section, circuits are compared in term, efficiency, robustness, step-up ratio, control and cost.

Efficiency

Top1 (and top2) show global efficiency of 80.6% (under typical Rint=9Ω). Loss analysis are identical to the boost and flyback standard circuits they are derived from, except for additional switching losses due to the self-oscillating circuits. Low switching frequency enables decrease of switching losses at

the expense of a large transformer magnetization inductance. Most losses are therefore located in diode D_1 and can be decreased with the addition of a parallel MOS transistor (at the cost of circuit complexity). The transformer used is chosen for its very low serial resistance and ensures low conductive losses at the expense of size. Figure 11 shows how global efficiency is impacted by internal resistance of MFCs.

Top3 can be customized according to different specifications. If C_3 is high compared to other circuit capacitors, it favors power transfer to the load. Top3 achieves 66.5% global efficiency (Rint=9Ω, C_3=8nF) but the circuit stops working if Rint increases above 9Ω. If C_3=2nF, top3 operates under Rint values up to 30Ω. In this case, the global efficiency is 41% only (Rint=9Ω).

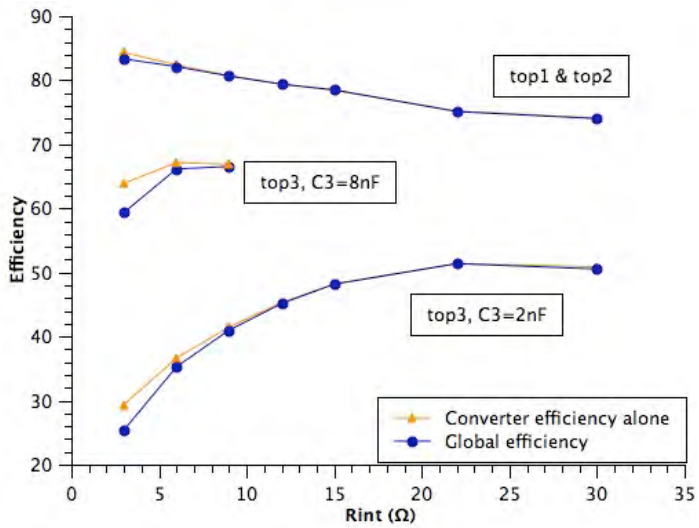

Fig. 11: Converter input and output voltages for different MFC internal resistance

Robustness

The sensitivity to key circuit parasitic parameters was studied. One of the main outcome is that the flyback topology (which is subject to current discontinuities) is very sensitive to the transformer leakage inductances because it creates detrimental high-frequency oscillations (global efficiency η=68% for coupling K=0.990 compared to the normal η=80.6% for coupling K=0.999). In this regard, the boost converter is more stable (global efficiency η=79% for coupling K=0.990 compared to the normal η=80.6% for coupling K=0.999).

Step-up

Boost efficiency theoretically decreases when the step-up ratio is high (duty cycle D>0.9). It is not verified with top1, probably due to the low switching frequency. Top2 and top3 benefit from the high transformer turn-ratio and theoretically enable higher step-up ratios.

Control

Top1 and top2 include a regulation loop which is designed to regulate the input voltage (enabling therefore the implementation of MPPT function). Top3 is unregulated. The input voltage is function of output load, and internal components sizing. It is possible to size it properly for given specifications, but the global efficiency decreases in case of large variation of MFC internal resistance (figure 11).

Cost

The 3 circuits are area consuming because of the large inductive elements they require for operation. Integration of active parts would decrease switching losses, enable higher frequency operation, and decrease constraints on inductive components.

Conclusion

Three low-voltage, low-power, high step-up DC:DC converter topologies were presented. They are optimized for energy harvesting from microbial fuel cells. Topologies are simulated with basic

electrical models of MFCs, ensuring a realistic comparison. The 3 topologies are analyzed and compared in term of global efficiency, robustness, step-up ratio, control and cost (table VI). A multi-criteria comparison shows that the modified boost topology (top1) is the best. Future works will be dedicated to experimentation.

Table VI: Comparison of studied harvesting DC:DC converters

	Efficiency	Robustness	Step-up	Control	Cost
Top1	80.6 %	good	average	good	high
Top2	80.6 %	bad	high	good	very high
Top3	66.5 %	good	high	none	average

References

[1] S. Roundy, D. Steingart, L. Frechette, and P. Wright, J, "Power sources for wireless sensor networks," *Sensor Networks*, vol. 2920, 2004, pp. 1-17.

[2] R.J.M. Vullers, R. van Schaijk, I. Doms, C. Van Hoof, and R. Mertens, "Micropower energy harvesting," *Solid-State Electronics*, vol. 53, Jul. 2009, pp. 684-693.

[3] S.T. Oh, J.R. Kim, G.C. Premier, T.H. Lee, C. Kim, and W.T. Sloan, "Sustainable wastewater treatment: How might microbial fuel cells contribute.," *Biotechnology advances*, Aug. 2010.

[4] I. Ieropoulos, J. Greenman, and C. Melhuish, "Improved energy output levels from small-scale Microbial Fuel Cells.," *Bioelectrochemistry (Amsterdam, Netherlands)*, vol. 78, Apr. 2010, pp. 44-50.

[5] J.W. Kimball, T.L. Flowers, S. Member, and P.L. Chapman, "Low-Input-Voltage , Low-Power Boost Converter Design Issues," *Power Electronics Letters*, vol. 2, 2004, pp. 96-99.

[6] P.-hung Chen, K. Ishida, X. Zhang, Y. Okuma, Y. Ryu, M. Takamiya, and T. Sakurai, "0 . 18-V Input Charge Pump with Forward Body Biasing in Startup Circuit using 65nm CMOS," *Small*, 2010, pp. 2-5.

[7] Y.K. Ramadass and A.P. Chandrakasan, "A batteryless thermoelectric energy-harvesting interface circuit with 35mV startup voltage," *Energy*, IEEE, 2010, p. 486–487.

[8] J.M. Damaschke, "Design of a low-input-voltage converter for thermoelectric generator," *IEEE Transactions on Industry Applications*, vol. 33, 1997, pp. 1203-1207.

[9] S. Ben-Yaakov and I. Fridman, "SPICE compatible model of self-oscillating converter," *Electrical and Electronics Engineers in Israel, 2004. Proceedings. 2004 23rd IEEE Convention of*, IEEE, 2004, p. 342–345.

[10] M. Pollak, L. Mateu, and P. Spies, "Step-up DC-DC-Converter with coupled inductors for low input voltages," *Fraunhofer IIS*, 2008.

[11] D. Grgić, T. Ungan, M. Kostić, and L.M. Reindl, "Ultra-low input voltage DC-DC converter for micro energy harvesting," *PowerMeMs*, 2009, pp. 265-268.

[12] Linear Technology, "Ultralow Voltage Step-Up Converter and Power Manager," *LTC3108 datasheet*, 2010, pp. 1-20.

[13] Coilcraft, "Coupled Inductors - LPR6235," *LPR6235 datasheet*, 2010, pp. 1-2.

[14] A. Anders, "ECT 310 – Powering from temperature difference," *WHITE PAPER*, 2010.

[15] Seiko, «Ultra-low voltage operation charge pump IC for step-up DC-DC converter startup», *S-882Z datasheet*, 2010

[16] Y. Qiu, C. Van Liempd, B.O. het Veld, P.G. Blanken, and C. Van Hoof, *5µW-to-10mW input power range inductive boost converter for indoor photovoltaic energy harvesting with integrated maximum power point tracking algorithm*, IEEE, 2011.

[17] F. Zhao, R.C.T. Slade, and J.R. Varcoe, "Techniques for the study and development of microbial fuel cells: an electrochemical perspective.," *Chemical Society reviews*, vol. 38, 2009, pp. 1926-39.

[18] G.C. Premier, J.R. Kim, I. Michie, R.M. Dinsdale, and A.J. Guwy, "Automatic control of load increases power and efficiency in a microbial fuel cell," *Journal of Power Sources*, Oct. 2010.

[19] Y. Zeng, Y.F. Choo, B.-H. Kim, and P. Wu, "Modelling and simulation of two-chamber microbial fuel cell," *Journal of Power Sources*, vol. 195, 2010, pp. 79-89.

[20] Z. Pei-yuan and L. Zhong-liang, "Experimental study of the microbial fuel cell internal resistance," *Journal of Power Sources*, Jun. 2010.